Free vibrations of an uncertain energy pumping system

Edson Cataldo, Sergio Bellizzi, Rubens Sampaio

Free vibrations of an uncertain energy pumping system

Edson Cataldo[a], Sergio Bellizzi[b], Rubens Sampaio[c]

[a] *Universidade Federal Fluminense, Applied Mathematics Departament and Graduate program in Telecommunications Engineering, Rua Mário Santos Braga, S/N, Centro, Niteroi, RJ, CEP: 24020-140, Brazil*
[b] *LMA, CNRS, UPR 7051, Centrale Marseille, Aix-Marseille Univ, F-13402 Marseille Cedex 20 France*
[c] *PUC-Rio, Mechanical Engineering Departament, Rua Marquês de São Vicente, 225, Gavea, Rio de Janeiro, RJ, CEP: 22453-900, Brazil*

Abstract

The aim of this paper is to study the energy pumping (the irreversible energy transfer from one structure, linear, to another structure, nonlinear) robustness considering the uncertainties of the parameters of a two DOF mass-spring-damper, composed of two subsystems, coupled by a linear spring: one linear subsystem, the primary structure, and one nonlinear subsystem, the so-called NES (non-linear energy sink). Three parameters of the system will be considered as uncertain: the nonlinear stiffness and the two dampers. Random variables are associated to the uncertain parameters and probability density functions are constructed for the random variables applying the Maximum Entropy Principle. A sensitivity analysis is then performed, considering different levels of dispersion, and conclusions are obtained about the influence of the uncertain parameters in the robustness of the system.

Key words: Energy pumping, uncertainties, modelling, dynamical system.

1. Introduction

Energy pumping (EP) refers to a mechanism in which energy is transferred in an one-way irreversible fashion from a source to a receiver. In the context of passive vibration control of mechanical systems, it can be used to develop a nonlinear dynamic absorber. In this case, the energy pumping occurs from the main, or primary, structure, which needs to be protected, to the nonlinear absorber coupled with it. The nonlinear absorber, also named Nonlinear Energy Sink (NES), consists of a mass with an essential nonlinear spring. This concept involves nonlinear energy interactions which occur due to internal resonances making possible irreversible nonlinear energy transfers from the primary system

Email addresses: ecataldo@im.uff.br (Edson Cataldo), bellizzi@lma.cnrs-mrs.fr (Sergio Bellizzi), rsampaio@puc-rio.br (Rubens Sampaio)

to the attachment. The nonlinear energy pumping in nonlinear mechanical systems was first described in [3, 17]. An important characteristic of the nonlinear dynamic absorber should be highlighted: since the NES is essential nonlinear, this system has no (or very small) natural frequency and it is effective for a large range of frequencies, while the linear absorbers attenuate well only one frequency. The linear system to which the NES is attached has, of course, a natural frequency. A complete description of the energy pumping phenomenon can be found in [18].

The energy pumping phenomenon has been studied extensively in deterministic frameworks including theoretical, numerical and experimental investigations. Very few studies have been devoted to analyze it in stochastic cases. Stochasticity was taken into account to discuss the robustness of energy pumping. In [7], the robustness of a nonlinear energy sink during transient regime was analyzed assuming various parameters as Gaussian random variables and using polynomial chaos expansion. In [14], the robustness was considered with respect to the initial condition and external excitation forces. Assuming Gaussian initial condition and white-noise excitation forces, the problem was analyzed solving the associated Fokker-Planck equation. In [13], a general linear system connected with an essentially nonlinear attachment in the presence of stochastic excitation to both the linear system and the nonlinear attachment and with random initial conditions was considered. The problem was analyzed combining the complexification-averaging technique and solving the Fokker-Planck-Kolmogorov equation associated to the slow dynamics of the system.

In this paper, uncertain parameters are considered and random variables are associated to them as in [7]. However, the corresponding probability density functions are constructed using the Maximum Entropy Principle [9]. This principle states that out of all probability density distributions consistent with the given set of available information, the one with the maximum uncertainty (entropy) must be chosen. Next, the robustness is investigated from the probabilistic properties of some quantities that measure the transfer of energy between the primary system to the NES. We focus on the ratio of the sum of the energy stored and energy dissipated in the primary system and sum of the energy stored and energy dissipated in the NES. This ratio can be related to the percentage of energy dissipated by the NES.

This paper is organized as follows: in Section 2, the deterministic model used to study the energy pumping phenomenon is introduced and the energy quantity used to analyze the transfer of energy is described. The stochastic approach used is described in Sec. 3. In Section 4, the robustness of the system is discussed taking into account the uncertainties of the parameters. A special case, considering the situation where the maximum of the energy pumping is obtained, is showed in Sec. 5. Finally, in Sec. 6 conclusions are outlined.

2. The deterministic model used

The system used to illustrate the energy pumping phenomenon and to discuss its robustness, taking into account uncertainties, has two-degrees-of-freedom and its sketch is shown in Fig. 1.

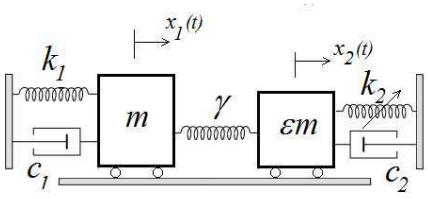

Figure 1: Energy pumping model.

The system is composed of two subsystems (mass-spring-damper) coupled by a linear stiffness. The first subsystem, corresponding to the linear part (or primary system), is composed of the mass m, the linear spring k_1 and the linear damping c_1. It defines a linear oscillator. The second subsystem, corresponding to the NES, is composed of a mass, which is proportional to m (ϵm), the cubic spring k_2 and the linear damping c_2. It defines a nonlinear oscillator. A linear spring γ couples the two subsystems. This configuration is referred as the grounded configuration because the NES is connected to the ground. This configuration has been considered in many studies to analyze the EP phenomenon in terms of transient dynamics [3, 6, 19], in terms of steady state dynamics [8, 12] and in experimental context [1, 12].

The equations of motion are given by Eq. 1:

$$\begin{cases} m\ddot{x}_1 + c_1\dot{x}_1 + k_1x_1 + \gamma(x_1 - x_2) = 0 \\ \epsilon m\ddot{x}_2 + c_2\dot{x}_2 + k_2x_2^3 + \gamma(x_2 - x_1) = 0 \end{cases} \tag{1}$$

where $x_1(t)$ and $x_2(t)$ denote the displacements of the primary system and the NES, respectively. Only free responses associated to impulsive excitation of the primary system will be analyzed, which corresponds to the following initial conditions:

$$x_1(0) = 0,\ \dot{x}_1(0) = \sqrt{\frac{2h}{m}},\ x_2(0) = 0 \text{ and } \dot{x}_2(0) = 0\ , \tag{2}$$

where h corresponds to the initial energy given to the system. This conditions may be given applying an impulse in the primary system. That is, some energy is introduced in the primary system at $t = 0$ and one sees how the energy is dissipated, if by the primary system or by the attachment.

As it is well known, energy pumping occurs when the value of the initial injected energy h is above a specific value [10]. The critical energy level (or pumping threshold) can be estimated from the Nonlinear Normal Modes (NNM) of the undamped associated nonlinear mechanical system using the frequency-energy-plot[11]. One NNM corresponds to periodic orbits where the oscillations

of the primary system (x_1) and the NES (x_2) are out of phase the other NNM corresponding to in phase oscillations. The energy pumping phenomenon happens through a nonlinear beat phenomenon activating a 1:1 internal resonance: x_1 and x_2 oscillate at the same frequency according to the in phase NNM where the motion is localized in the NES. This state permits the transfer of the energy from the linear subsystem to the NES where the energy is dissipated (transfer in a irreversible way)[11].

The transfer of energy can be analyzed observing the energy exchanged between the two subsystems and/or comparing the energy dissipated by the two subsystems. This approach will be considered here.

As in [6], the following energy quantities are introduced

$$E_1(t) = \frac{1}{2}m\dot{x}_1^2(t) + \frac{1}{2}k_1x_1^2(t) + c_1\int_0^t \dot{x}_1^2(s)ds \tag{3}$$

$$E_2(t) = \frac{1}{2}\epsilon m\dot{x}_2^2(t) + \frac{1}{4}k_2x_2^4(t) + c_2\int_0^t \dot{x}_2^2(s)ds \tag{4}$$

where $E_i(t)$ denotes the sum of the mechanical energy present in the subsystem i at time t and the energy dissipated in the subsystem i over $[0,t]$. At $t=0$, $E_i(0)$ corresponds to the energy introduced in the subsystem i and at $t=+\infty$, $E_i(+\infty)$ corresponds to the energy dissipated in the subsystem i. Note that with the imposed initial conditions (2), $E_1(0)=h$ and $E_2(0)=0$.

Starting from the equations of motion (1) and using the initial conditions (2), it can be shown that the non dimensional ratio $r_E(t)=\dfrac{E_2(t)}{E_1(t)}$ (also named energy ratio) reduces to

$$r_E(t) = \frac{-\displaystyle\int_0^t \dot{x}_1(s)x_2(s)ds - \tfrac{1}{2}x_2^2(t)}{\tfrac{h}{\gamma} + \displaystyle\int_0^t \dot{x}_1(s)x_2(s)ds - \tfrac{1}{2}x_1^2(t)} \tag{5}$$

giving

$$r_E(0)=0 \text{ and } r_E(+\infty) = \frac{-\displaystyle\int_0^{+\infty} \dot{x}_1(s)x_2(s)ds}{\tfrac{h}{\gamma} + \displaystyle\int_0^{+\infty} \dot{x}_1(s)x_2(s)ds}. \tag{6}$$

The non dimensional ratio $r_E(+\infty)$ is also related to the percentage of energy dissipated by the subsystem 2 (the NES) over $[0,+\infty]$ as

$$\frac{E_2^{dis}}{E_1^{dis}+E_2^{dis}} = \frac{r_E(+\infty)}{1+r_E(+\infty)} \tag{7}$$

where E_i^{dis} denotes the energy dissipated in the subsystem i over $[0,+\infty]$.

When energy is transferred from the primary system to the NES, $E_2(t)$ can become greater than $E_1(t)$ giving $r_E(t) > 1$. Hence, energy pumping occurs if there exists T_p such that $r_E(t) \geq 1$ for all t, $t \geq T_\mathrm{p}$. Note that $r_E(t) \geq 1$ can also occur for $t < T_\mathrm{p}$.

Energy pumping will be efficient if T_p is small and $r_E(+\infty)$ is large (always greater than 1). The last condition will be satisfied if the denominator of (6) is near zero corresponding to a negative value for the integral $\int_0^{+\infty} \dot{x}_1(s)x_2(s)ds$. This condition will mainly occur during the activation of a 1:1 internal resonance (the energy pumping phase) where the components $x_1(t)$ and $x_2(t)$ are in-phase (see previous comment and [1]). In this paper, treating the free vibration problem, it will be studied the conditions that assure energy pumping, but not its effectiveness. In a follow-up problem dealing with forced vibrations, where a primary system is to be protected using a NES, it would be more interesting to study also the effectiveness of the energy pumping, connected with the value of T_p.

Typical behaviors of the non dimensional ratio $r_E(t)$ versus time are plotted in Fig. 2 for $m = 1$ kg, $\epsilon = 0.1$, $k_1 = 0.9$ N m^{-1}, $k_2 = 0.1$ N m^{-3}, $\gamma = 0.05$ N m^{-1}, $c_1 = 0.05$ N s m^{-1} and $c_2 = 0.01$ N s m^{-1}. Three values ($h = 0.01, 0.15$ and 1) of the initial energy will be considered showing that in these cases energy pumping only occurs for $h = 0.15$.

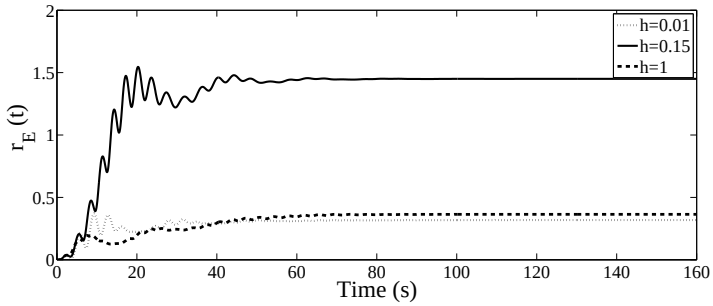

Figure 2: Energy ratio r_E versus time t, considering three different cases for the initial energy: $h = 0.01$ (dotted line), $h = 0.15$ (dashed line) and $h = 1$ (continuous line).

For the same set of numerical values, the behavior of the $r_E(t)$ at $t = +\infty$ versus the initial energy h is plotted (Fig. 3).

When h is small, no energy pumping occurs ($r_E(+\infty) < 1$). When $h \geq h_\mathrm{p}^\mathrm{i}$ where h_p^i is defined as the initial energy where the curve $r_E(+\infty)$ cross up the horizontal line $y = 1$ (here $h_\mathrm{p}^\mathrm{i} \approx 0.09$ as seen in Fig. 3), the energy pumping occurs ($r_E(+\infty) \geq 1$). Increasing h, the energy pumping phenomenon disappears for $h \geq h_\mathrm{p}^\mathrm{f}$ where h_f^i is defined as the initial energy where the curve $r_E(+\infty)$ cross down the horizontal line $y = 1$ (here $h_\mathrm{p}^\mathrm{f} \approx 0.25$ as seen in Fig. 3). For the selected configuration, the energy pumping is optimal for $h \approx 0.15$ and in this case the NES dissipates 60% of the energy.

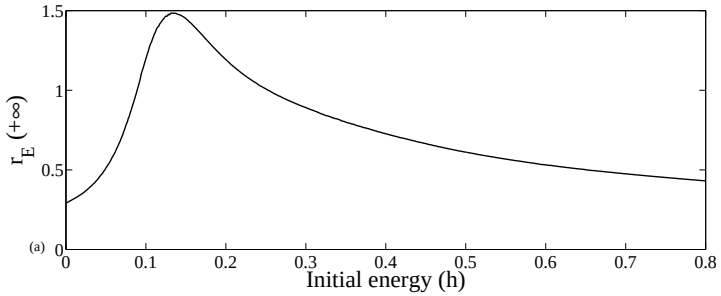

Figure 3: Energy ratio $r_E(t)$ at $t = +\infty$ versus initial energy h.

The threshold value $h_{\mathrm{p}}^{\mathrm{i}}$ can be compared to the pumping threshold estimated from the nonlinear normal modes of the undamped associated nonlinear mechanical system. The two nonlinear normal modes have been computed using the complexification-averaging method [18]. They are depicted using the energy-frequency-plot (see Fig. 4(a)) and the displacement-frequency plots (see Fig. 4(b)). The energy is defined as

$$\text{Energy} = \frac{1}{2}m\dot{x}_1^2 + \frac{1}{2}\epsilon m\dot{x}_2^2 + \frac{1}{2}k_1x_1^2 + \frac{1}{2}\gamma(x_1 - x_2)^2 + \frac{1}{4}k_2x_2^4.$$

The first NNM corresponds to in-phase periodic orbits (Fig. 4, gray curves). The second NNM corresponds to out-of-phase periodic orbits (Fig. 4, black curves). The pumping threshold is defined as the energy value where the out of phase NNM shows a local maximum (see the horizontal line (Fig. 4(a)). The value (≈ 0.08) is close to $h_{\mathrm{p}}^{\mathrm{i}} \approx 0.09$.

Considering a deterministic system, it was possible to discuss the principles of the energy pumping. However, the main objective here is to discuss the robustness of energy pumping taking into account the uncertainties of some parameters of the system; that is, to discuss what happens with the energy pumping phenomenon when the parameters of the system are uncertain. Random variables will be associated to these parameters and the corresponding stochastic system constructed.

3. The stochastic approach used

3.1. General considerations

In order to apply the theory to real structures, where the nonlinear structure annexed does not reflect perfectly the theoretical conception and the problems related to the nonlinear identification appear, it is important to know if the energy pumping can be produced even when the parameters are uncertain. The aim of this section is to study the energy pumping when uncertainties are present; that is, when the values of the parameters are not well known.

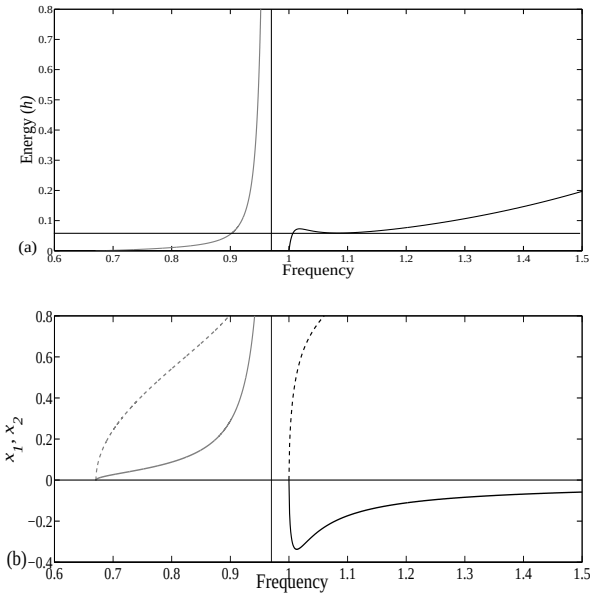

Figure 4: Nonlinear normal modes of the undamped associated nonlinear mechanical system in terms of (a) energy-frequency-plot and (b) displacement-frequency-plot. In phase NNM (gray curves), out of phase NNM (black curves). x_1 component (continuous lines), x_2 component (dashed lines)

.

3.2. Stochastic modeling

Herein, the most relevant parameters in terms of energy pumping have be chosen as uncertain: (i) k_2, the nonlinear stiffness, (ii) c_1, the damping corresponding to the linear system, and (iii) c_2 the damping corresponding to the nonlinear system. The nonlinear energy pumping occurs if the damping of the NES and damping of the primary system are small[4], inceasing one of these parameters can cancel the energy transfer. As shown by energy-frequency-plot representation of the NNMs, the pumping threshold is also strongly related to the nonlinear stiffness coefficient of the NES. This set of parameters also correspond to the quantities that are difficult to characterize in practice.

To construct the corresponding stochastic model, random variables K, C_1 and C_2 will be associated to the uncertain parameters and probability density functions constructed to these random variables using the Maximum Entropy Principle [9].

Let Y be each one of the random variables K, C_1 or C_2. If p_Y is the probability distribution of Y, the entropy associated to Y is defined by [16]:

$$S(p_Y) = -\int_{-\infty}^{+\infty} p_Y(y)\ell n(p_Y(y))dy. \tag{8}$$

The goal is to maximize S under the constraints defined by some available information on the random variable Y.

For our problem, the following information is considered as available: (i) the support of the probability density function is $]0, +\infty[$, (ii) the mean value, which is known, $E[Y] = \underline{Y}$ and (iii) the condition $E\{\ell n(Y)\} < +\infty$ which implies that zero is a repulsive value.

The probability density function p_Y has then to verify the following constraint equations [2]:

$$\int_{-\infty}^{+\infty} p_Y(y)dy = 1 \ , \ \int_{-\infty}^{+\infty} y p_Y(y)dy = \underline{Y} \ , \ \int_{-\infty}^{+\infty} \ell n(Y) p_Y(y)dy < +\infty \, . \quad (9)$$

Applying the Maximum Entropy Principle yields the following probability density function for Y:

$$p_Y(y) = \mathbf{1}_{]0,+\infty[}(y) \frac{1}{\underline{Y}} \left(\frac{1}{\delta_Y^2} \right)^{\frac{1}{\delta_Y^2}} \times \frac{1}{\Gamma\left(1/\delta_Y^2\right)} \left(\frac{y}{\underline{Y}} \right)^{\frac{1}{\delta_Y^2}-1} exp\left(-\frac{y}{\delta_Y^2 \underline{Y}} \right) \quad (10)$$

where $\delta_Y = \dfrac{\sigma_Y}{\underline{Y}}$ is the coefficient of dispersion of the random variable Y such that $\delta_Y < \dfrac{1}{\sqrt{2}}$ and σ_Y is the standard deviation of Y.

It can be verified that Y satisfies

$$E\{1/Y^2\} < +\infty \, . \quad (11)$$

3.3. Stochastic solver for the uncertain system

The stochastic system is constructed from the corresponding deterministic one substituting k_2, c_1 or c_2 by the random variable K, C_1 or C_2, respectively. The stochastic solver used is based on the Monte Carlo method. Each random variable will be substituted separately by the corresponding uncertain parameter in the deterministic system.

The following steps will be performed for each random variable.

(i) A probability density function is constructed using the Maximum Entropy Principle (see previous section).

(ii) Independent realizations $Y(\theta)$ of the random variable Y are constructed using the associated probability density function obtained in step (i). For each realization $Y(\theta)$, the system of differential equations given by Eqs. (1)(2) is numerically solved and the stochastic processes $X_1(t)$ and $X_2(t)$, associated to the displacements $x_1(t)$ and $x_2(t)$ of the masses m_1 and m_2, are obtained.

(iii) Confidence intervals corresponding to different quantities related to the energy pumping phenomenon (such as nonlinear normal modes, r_E,...) are

plotted considering different values for the dispersion coefficient. The confidence interval associated with a specific probability level is constructed using quantiles [2, 15]. Herein, the probability that one realization is inside the confidence interval is 0.95.

4. Energy pumping robustness

The following numerical values have been used to define the nominal system: $m = 1$ kg, $\epsilon = 0.1$, $k_1 = 0.9$ N m^{-1}, $k_2 = 0.1$ N m^{-3}, $\gamma = 0.05$ N m^{-1}, $c_1 = 0.05$ N s m^{-1} and $c_2 = 0.01$ N s m^{-1}. The equations of motion Eq. (1)(2) have been approximated over $[0, T]$ with $T = 160\,s$ using Runge-Kutta method. The confidence intervals have been estimated simulating 200 realizations.

4.1. Parameter k_2 chosen as uncertain

The nonlinear stiffness k_2 is considered as uncertain. The probability density function of the associated random variable K is defined from (10) with $Y = K$. It is assumed that $E[K] = \underline{K} = k_2$.

From the relation (11), it can be deduced that $E\{1/K^{2/3}\} < +\infty$. Let X be the random variable corresponding to a displacement of the stiffness k_2 and let F be the force applied to k_2. Then, $F = KX^3$. Therefore, $E\{X^2\} < +\infty \Rightarrow E\{1/K^{2/3}\} < +\infty$.

Figure 5 shows the confidence interval of the displacement of the nonlinear normal modes (considered as the conserved mechanical energy of the associated periodic orbits) in relation to the frequency, when the dispersion coefficient varies. It is also reported the evolution of the mean values of the realizations and energy-frequency plot associated to the nominal systems. It can be noted that the mean values of the realizations slightly differ from the results obtained from the nominal system. However, the uncertainty on k_2 affects differently the nonlinear normal modes. For the out-of-phase branch, the influence of the uncertainty increases with the frequency affecting significantly the pumping threshold. For the in-phase branch, the uncertainty affects the branch where the curvature is larger.

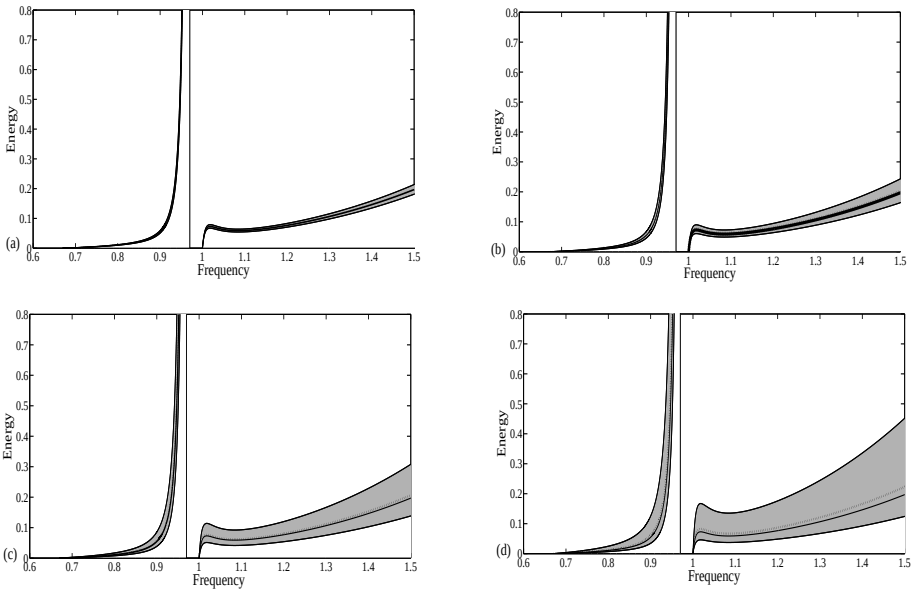

Figure 5: Confidence interval related to the displacements of the nonlinear normal modes (considered as the conserved mechanical energy of the associated periodic orbits) and the mean values of the realizations (dashed line) for different values of the dispersion coefficient δ_K of the random variable K, : (a) $\delta_K = 0.05$, (b) $\delta_K = 0.1$, (c) $\delta_K = 0.2$ and (d) $\delta_K = 0.3$. Energy-frequency-plot of the nominal system (thick line).

Figure 6 shows the confidence interval of the energy ratio $r_E(t)$ at $t = +\infty$ in relation to the variation of the initial energy $h \in [0, 0.8]$ when the dispersion coefficient varies.

The scale of the plots was chosen so that the results can be compared with other confidence intervals that will be constructed in the following. The uncertainty on k_2 affects $r_E(+\infty)$ over $h \in [0, 0.8]$. When the dispersion coefficient

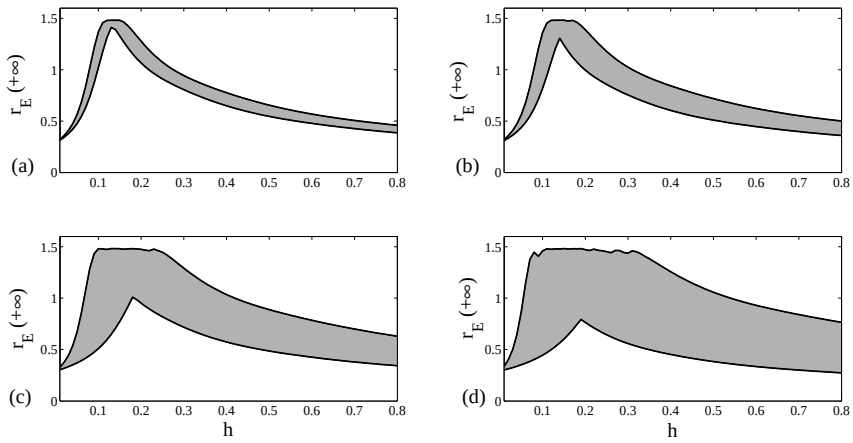

Figure 6: Confidence interval related to the energy ratio $r_E(t)$ at $t = +\infty$ versus initial energy h for different values of the dispersion coefficient of the random variable K. (a) $\delta_K = 0.05$. (b) $\delta_K = 0.1$. (c) $\delta_K = 0.2$. (d) $\delta_K = 0.3$

is small, the phenomenon of energy pumping is robust for a large initial energy range. Increasing the dispersion, the initial energy range corresponding to the energy pumping is reduced and for $\delta_K = 0.3$ the robustness of the energy pumping phenomenon is lost. These curves show also a very interesting result concerning the influence of the uncertainty of k_2 on the efficiency of the NES. The upper-bound of the confidence interval shows an upper-bound (≈ 1.4) and remains equal to this value in the energy pumping range. It indicates that the energy pumping efficiency cannot be increased varying only K. There is a limit for it.

The energy pumping robustness can also be analyzed for a given initial energy. Figure 7 shows the realizations of the displacements of the two masses with the initial energy $h = 0.15$ considering $\delta_K = 0.3$ as the value of the dispersion coefficient.

Here, basically, the same characteristics obtained by [5] can be highlighted. The energy pumping phenomenon is produced and it is effective for all the realizations (Fig. 7 (a) and (b)). The mean values of $x_1(t)$ and $x_2(t)$ (Fig. 7 (c) and (d)) are characterized by two different behaviors: At the beginning, for $0 < t < 15\,s$, the mean displacements of the two oscillators are almost in-phase, the oscillation of the mean displacement of the NES is large and the decay of the primary system displacement is linear and very fast compared with that of the primary system disconnected from the NES (a one DOF linear oscillator) where the decay (not shown here) is exponential with decay rate 0.025. Then, for $t > 15$, the behavior of the two oscillators present out-of-phase displacements and the standard deviations of $x_1(t)$ and $x_2(t)$ are small, although near $t = 20s$ their values are higher. Figure 7 (e) and (f) show the standard

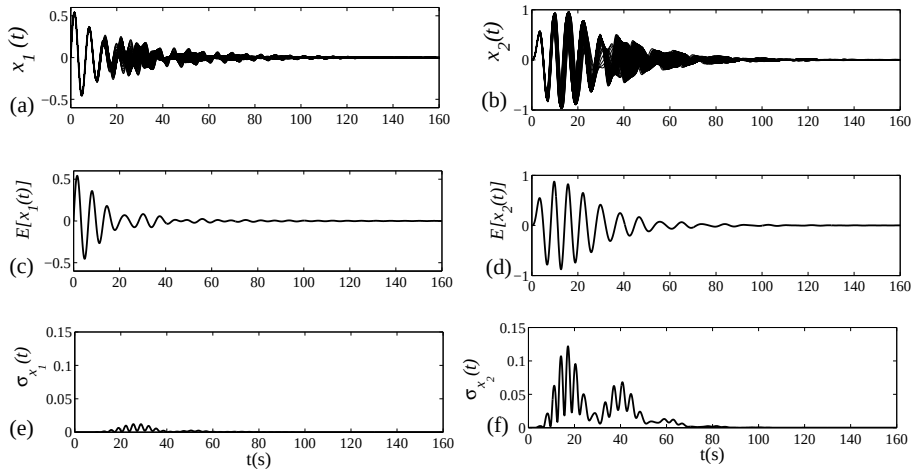

Figure 7: Numerical results for $\underline{K} = 0.1$ and $\delta_K = 0.3$. (a) and (b): Realizations of the displacements of the masses. (c) and (d): Mean values of the realizations. (e) and (f): Standard deviation of the realizations. Left: linear system. Right: nonlinear system.

deviation corresponding to the realizations.

Figure 8 shows the confidence interval of the energy ratio $r_E(t)$, with respect to time, when the dispersion coefficient varies. The scale of the plots was chosen so that the results can be compared with other confidence intervals that will be constructed in the following.

When the dispersion coefficient has a low value (0.05) it can be noted that all the realizations cross the value 1, approximately after the first 15 seconds, and remain above the value 1 during all the time indicating that the energy pumping occurs. Increasing the dispersion coefficient (0.1) it can be observed that the confidence interval is larger and some realizations remain under the value 1 during all the time, indicating that the energy pumping does not occur anymore. Increasing a little bit more the dispersion coefficient (0.2 and 0.3) more realizations appear under the value 1. Consequently, the energy pumping phenomenon is not effective, for these realizations.

Figure 9 shows the confidence interval of the energy ratio, with respect to time, considering only the coefficient of dispersion $\delta_K = 0.3$.

It can be noted that the nominal value and the mean value are not coincident. This happens due to the nonlinear characteristic of the system. To better understanding this behavior, a 3D graph was constructed and is shown in Fig. 10. The graph shows some realizations of K and the corresponding behavior of the energy.

It is important to note that the maximum value of the energy ratio occurs for values of K near to 0.07.

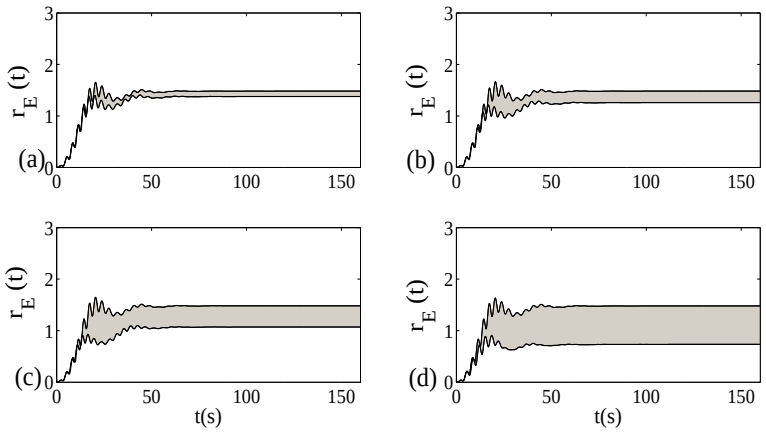

Figure 8: Confidence interval related to the energy ratio r_E versus time t for different values of the dispersion coefficient of the random variable K. (a) $\delta_K = 0.05$, (b) $\delta_K = 0.1$, (c) $\delta_K = 0.2$ and (d) $\delta_K = 0.3$.Initial energy $h = 0.15$.

4.2. Parameter c_1 chosen as uncertain

The next parameter to be considered as uncertain is the linear damping c_1 and the random variable C_1 will be assigned to it. The available information is the same as considered for K and, consequently, using the Maximum Entropy Principle, the corresponding probability density function constructed will have the same expression as the one constructed for K (Eq. 10), substituting K by C_1.

Figure 11 shows the confidence interval of the energy ratio in relation to the variation of the initial energy (h).

It can be noted that the maximum values of the energy ratio occurs for values of h near to 0.15.

The confidence interval for the realizations of the energy ratio is plotted for different values of the dispersion coefficient and the results are shown in Fig. 12.

In this case, the confidence interval seems to be considerable large when the value of the dispersion coefficient is $\delta_{C_1} = 0.3$ and, maybe, only in this case, the energy pumping cannot occur for some realizations. It indicates that the system is very robust in relation to variations of the uncertain parameter c_1. For all the other cases, the lower limit of the confidence interval is not below the level 1.

It is interesting to note that the confidence intervals considering C_1 as the only random variable is smaller than the one obtained when K was considered as the only random variable of the stochastic system.

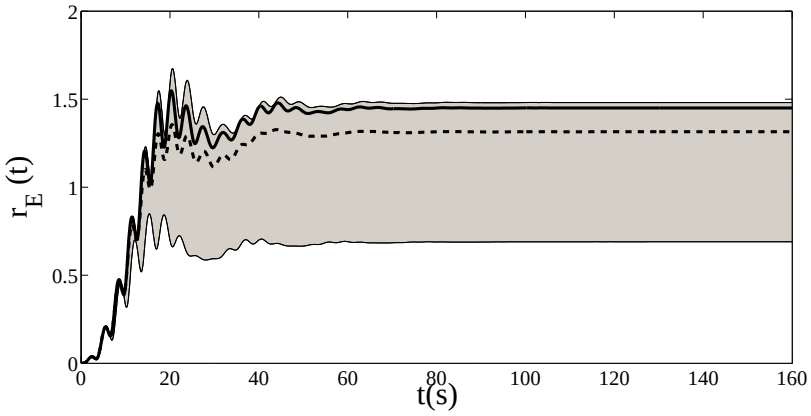

Figure 9: Confidence interval related to the energy ratio r_E versus time t considering $\delta_K = 0.3$, the nominal value (thick line) and the mean value (dashed line). Initial energy $h = 0.15$.

Figure 13 shows the particular case of the confidence interval in which $\delta_{C_1} = 0.3$, including the nominal and mean values of the energy ratio.

In this case, the graphs corresponding to the nominal and mean values for the energy ratio are almost the same and they are near the middle of the confidence interval. It is interesting to observe that this damping coefficient belongs to the linear part of the system. The confidence interval presented here is larger than the one shown in the Fig. 9, however the range below the level 1 is shorter.

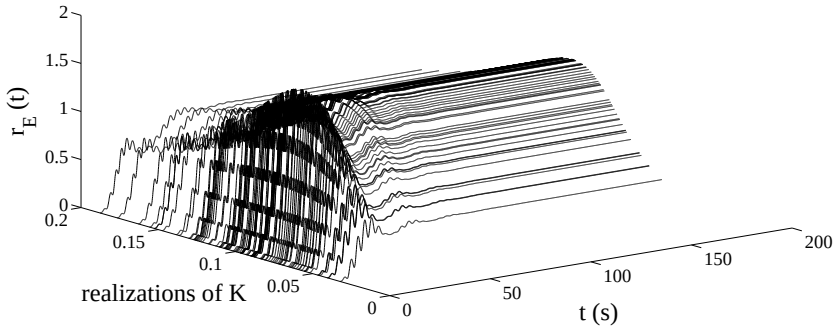

Figure 10: Realizations of the energy ratio in a 3D graph considering the values of K ordered, with $\delta_K = 0.3$.

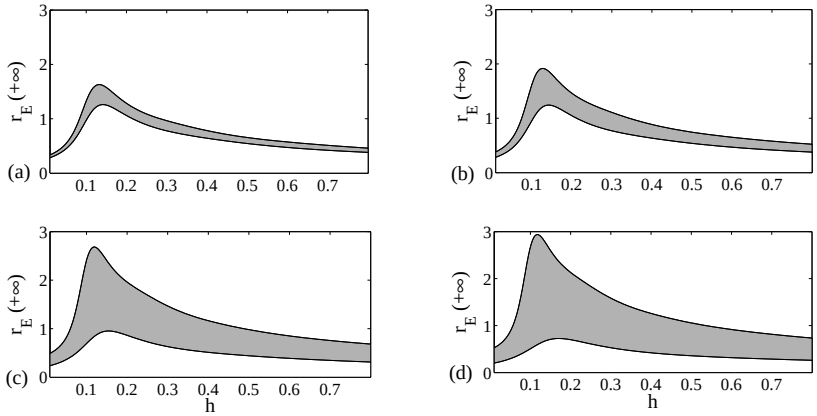

Figure 11: Confidence interval related to the energy ratio $r_E(t)$ at $t = +\infty$ versus initial energy h for different values of the dispersion coefficient of the random variable C_1. (a) $\delta_{C_1} = 0.05$. (b) $\delta_{C_1} = 0.1$. (c) $\delta_{C_1} = 0.2$. (d) $\delta_{C_1} = 0.3$

Figure 14 shows a 3D graph, considering some realizations of C_1, and the corresponding behavior of the energy ration was obtained.

This graph is particularly useful because it shows how the energy ratio changes when C_1 varies and also it shows the maximum value of the energy ratio, which occurs for values of C_1 near to 0.02, indicating a possible value for increasing the energy pumping.

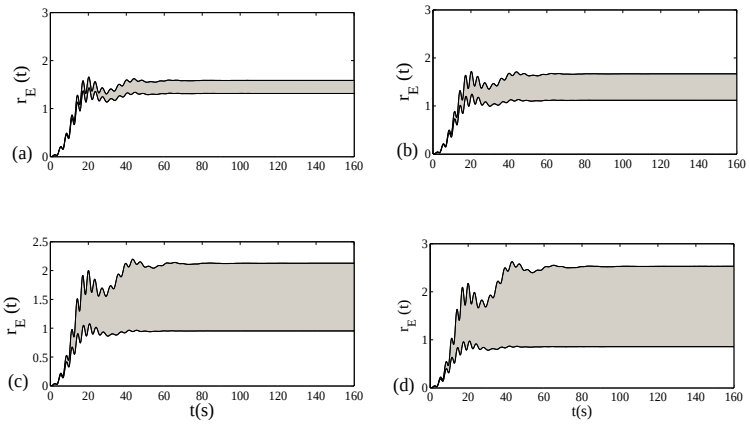

Figure 12: Confidence interval related to the energy ratio r_E versus time t for different values of the dispersion coefficient of the random variable C_1. (a) $\delta_{C_1} = 0.05$. (b) $\delta_{C_1} = 0.1$. (c) $\delta_{C_1} = 0.2$. (d) $\delta_{C_1} = 0.3$. Initial energy $h = 0.15$.

4.3. Parameter c_2 chosen as uncertain

The next parameter to be considered as uncertain is the linear damping c_2 associated to the nonlinear subsystem, and the random variable C_2 is assigned to it. The available information is the same as considered for C_1 and, consequently, using the Maximum Entropy Principle, the corresponding probability density function constructed will have the same expression as the one constructed for C_1 (and K) (Eq. 10), substituting C_1 (or K) by C_2.

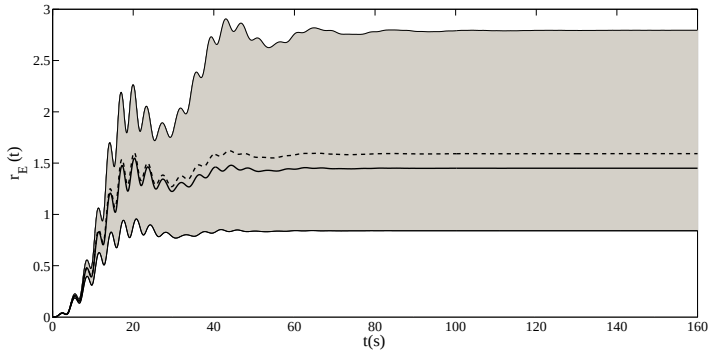

Figure 13: Confidence interval related to the energy ratio r_E versus time t considering $\delta_{C_1} = 0.3$, the nominal and mean values of the energy ratio. Initial energy $h = 0.15$.

Figure 15 shows the confidence interval of the energy ratio in relation to the variation of the initial energy (h).

It can also be noted that the energy ratio is maximum when h is near 0.15.

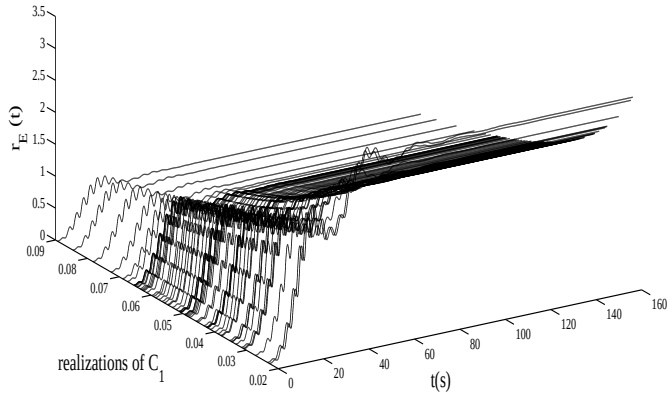

Figure 14: Realizations of the energy ratio in a 3D graph considering the ordered values of C_1, with $\delta_{C_1} = 0.3$.

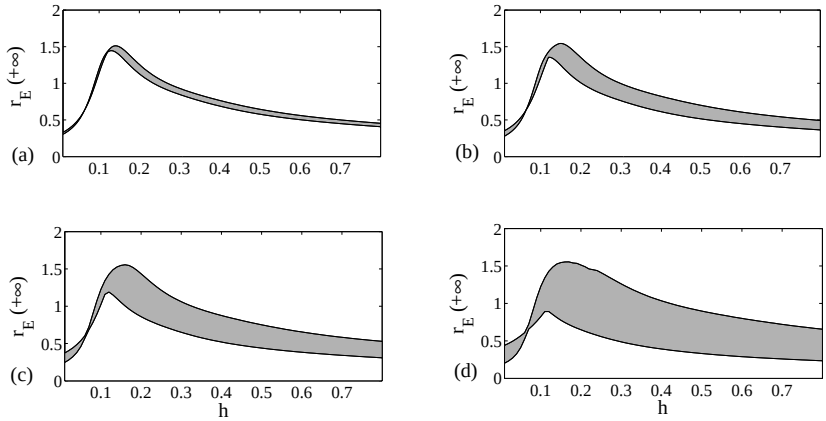

Figure 15: Confidence interval related to the energy ratio $r_E(t)$ at $t = +\infty$ versus initial energy h for different values of the dispersion coefficient of the random variable C_2. (a) $\delta_{C_2} = 0.05$. (b) $\delta_{C_2} = 0.1$. (c) $\delta_{C_2} = 0.2$. (d) $\delta_{C_2} = 0.3$

Figure 16 shows the confidence interval related to the energy ratio for different values of the dispersion coefficient δ_{C_2}.

One can say that the system is still robust considering the uncertainties of this parameter, but less robust when compared with values obtained when the random variable C_1 is considered.

Figure 17 shows the particular case of the confidence interval in which $\delta_{C_2} =$

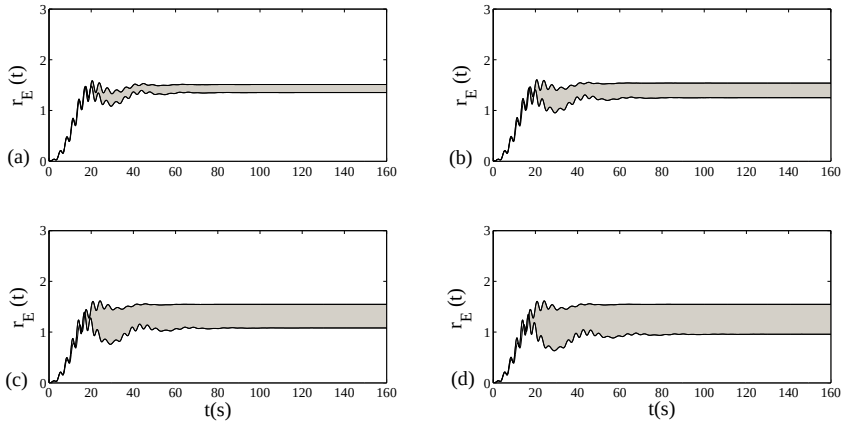

Figure 16: Confidence interval related to the energy ratio r_E versus time t for different values of the dispersion coefficient. (a) $\delta_{C_2} = 0.05$. (b) $\delta_{C_2} = 0.1$. (c) $\delta_{C_2} = 0.2$. (d) $\delta_{C_2} = 0.3$. Initial energy $h = 0.15$.

0.3, including the nominal and mean values of the energy ratio. Again, the mean and the nominal values for the energy ratio are not in the middle of the confidence interval, in the same way as it happened when K was considered as random variable. C_2 is the damping of the nonlinear part of the system.

Comparing the graph of Fig. 17 with the ones in Figs. 9 and 13 it can be noted that the confidence interval presented here is shorter than those ones. In addition, maybe it is not difficult to note that it shows less realizations below the level one than those ones. Then, one can risk saying that the system is more robust related to the parameter c_2 than the other two analyzed, k_2 and c_1. It means that, the variation of the energy ratio is less sensitive in relation to the variation of c_2 than k_2 and c_1.

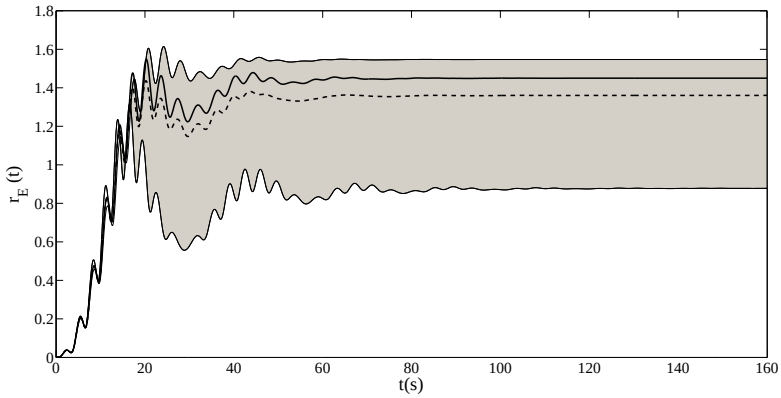

Figure 17: Confidence interval related to the energy ratio r_E versus time t considering $\delta_{C_2} = 0.3$, the nominal value (thick line) and mean value (dashed line) of the energy ratio. Initial energy $h = 0.15$.

Figure 18 shows a 3D graph containing some realizations of the energy ratio, in relation to time, obtained from realizations of C_2 when it is considered the only random variable of the system.

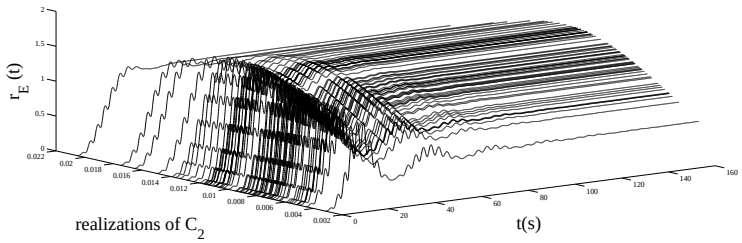

Figure 18: Realizations of the energy ratio in a 3D graph considering the values of C_2 ordered.

This graph help us to obtain the maximum value of the energy ratio, which occurs for values of C_2 near to 0.014, indicating which values of C_2 can be considered to increase the energy pumping.

4.4. The three parameters chosen as uncertain

Now, all the three uncertain parameters are considered in the stochastic system. Figure 19 shows the confidence interval of the energy ratio in relation to the variation of the initial energy (h).

It is interesting to note that, although the confidence interval has a limit, it is not a robust limit like with the variable K.

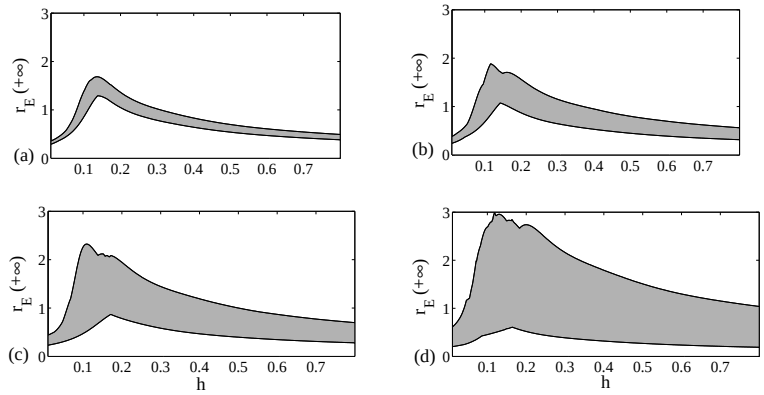

Figure 19: Confidence interval related to the energy ratio $r_E(t)$ at $t = +\infty$ versus initial energy h for different values of the dispersion coefficient of the random variables K, C_1 and C_2, with $\delta = \delta_K = \delta_{C_1} = \delta_{C_2}$. (a) $\delta = 0.05$. (b) $\delta = 0.1$. (c) $\delta = 0.2$. (d) $\delta = 0.3$

Figure 20 shows the confidence interval of the energy ratio in relation to time variation. Up to $\delta = 0.2$ many realizations are over the level 1 for the energy ratio. Only for $\delta = 0.3$ it can be seen more realizations below level 1 showing that the energy pumping does not occur.

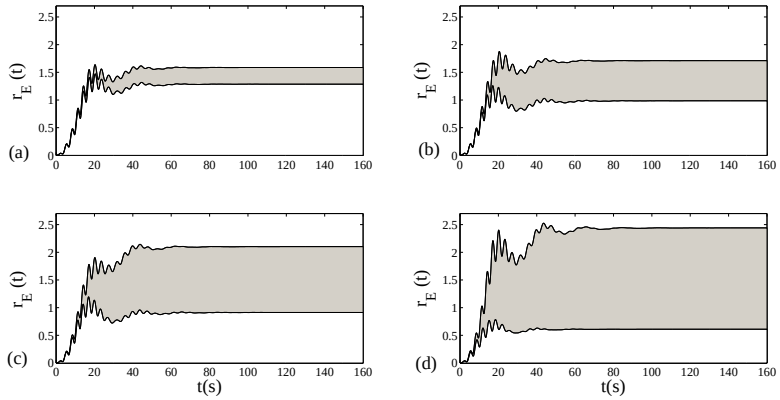

Figure 20: Confidence interval related to the energy ratio r_E versus time t for different values of the dispersion coefficient. (a) $\delta_K = \delta_{C_1} = \delta_{C_2} = 0.05$.(b) $\delta_K = \delta_{C_1} = \delta_{C_2} = 0.1$. (c) $\delta_K = \delta_{C_1} = \delta_{C_2} = 0.2$. (d) $\delta_K = \delta_{C_1} = \delta_{C_2} = 0.3$. Initial energy $h = 0.15$.

5. A special case

Considering all the study performed, mainly regarding the $3D$ graphs plotted, new values for the uncertain parameters were considered in order to try to obtain a greater value for the energy ratio, consequently greater energy pumping. The parameters were chosen so that the maximum values of the energy ratio were obtained. Two cases were considered, with two different values for k_2: 0.1 N m^{-3} and 0.07 N m^{-3}. The other values considered were $m = 1$ kg , $\epsilon = 0.1$, $k_1 = 0.9$ N m^{-1}, $\gamma = 0.05$ N m^{-1}, $c_1 = 0.025$ N s m^{-1} and $c_2 = 0.014$ N s m^{-1}. It is important to highlight that the values of k_2, c_1 and c_2 are the ones modified in relation to the values considered for the first simulation in this paper considering the deterministic case. Figure 21 shows the two plots.

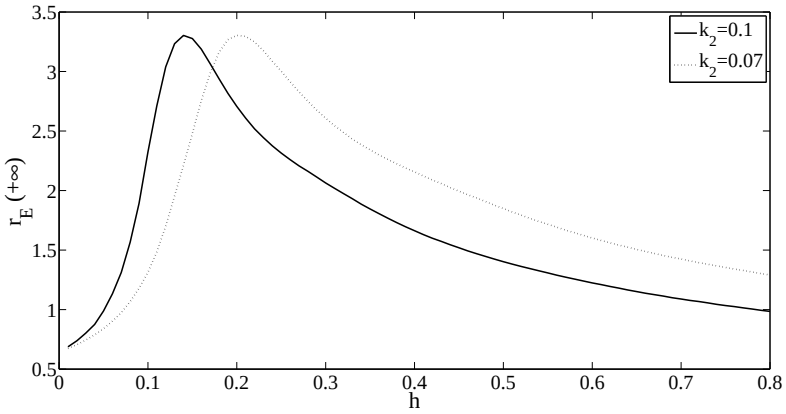

Figure 21: Energy ration $r_E(t)$ at $t = +\infty$ versus initial energy h in order to increase the value of the energy ratio.

It can be noted that the value of the energy non dimensional ratio was increased in both cases, comparing with the values obtained in the preceding sections. In the second case, with $k_2 = 0.07$, the maximum value of the energy ration (r_E) was obtained for h near to 0.25. This value is different from the one considered in all the simulations used in this paper. However, for the first case ($k_2 = 0.1$ N m^{-3}), the value of h corresponding to the maximum of the energy non dimensional ratio was near to 0.15. Then, it was possible to obtain a greater value for the energy ratio; that is, it was possible to increase the energy pumping, changing the values of the parameters and using all the study described in this paper.

6. CONCLUSIONS

This paper analyzes energy pumping using a system composed of two subsystems, one linear and another nonlinear, to take into account the uncertainties in some parameters. The main objective was to analyze the robustness of the energy pumping. So, three parameters were considered as uncertain: the nonlinear stiffness and the two damping, one of the linear subsystem and the other of the nonlinear subsystems. Probability density functions (p.d.f.) were assigned to the random variables related to these parameters.

The main conclusions obtained were that the system is more robust when uncertainties related to the dampers are taken into account, because with a greater level of dispersion in this parameter, the energy pumping phenomenon could still be observed. For the same level of dispersion, the effects of the three random variables were compared and the system results were more sensitive to variations of the random variable associated to the stiffness associated to the nonlinear system. In addition, the displacements of the linear subsystem are less sensitive to the variations of the uncertain parameter than the displacements of the nonlinear subsystem.

It was also possible to verify that, in some cases, there are limitation for the energy pumping. As an example, when only the stiffness associated to the nonlinear system was considered, it was not possible to increase the energy pumping varying the value of the random variable associated to the corresponding stiffness. However, it was possible to increase the energy pumping modifying the parameters of the system, according to all the study performed in the paper, considering the uncertain parameters, the random variables associated to them and the corresponding stochastic system.

An idea for a future study is to consider other parameters as uncertain and employ other methodologies to take it into account. The sensitive analysis can be performed considering Other quantities, for example, the energy variation of the system.

7. ACKNOWLEDGMENTS

This work was supported by FAPERJ (Fundação de Amparo à Pesquisa no Rio de Janeiro), by CAPES (CAPES/COFECUB project N. 672/10) and by CNPq (Brazilian Agency Conselho Nacional de Desenvolvimento Científico e Tecnológico).

References

[1] R. Bellet, B. Cochelin, P. Herzog, and P.-O. Mattei. Experimental study of targeted energy transfer from an acoustic system to a nonlinear membrane absorber. *Journal of Sound and Vibration*, 329:2768–2791, 2010.

[2] E. Cataldo, C. Soize, R. Sampaio, and C. Desceliers. Probabilistic modeling of a nonlinear dynamical system used for producing voice. *Computational Mechanics*, 43:265–275, 2009.

[3] O.V. Gendelman, L.I. Manevitch, A.F. Vakakis, and R. M'Closkey. Energy pumping in nonlinear mechanical oscillators: Part I - Dynamics of the underlying hamiltonian systems. *Journal of Applied Mechanics*, 68:34–41, 2001.

[4] E. Gourdon. *Controle passif de vibrations par pompage énergétique*. PhD thesis, Ecole Centrale de Lyon, 2006.

[5] E. Gourdon and C.H. Lamarque. Energy pumping for a larger span of energy. *Journal of Sound and Vibration*, 285:711–720, 2005.

[6] E. Gourdon and C.H. Lamarque. Energy pumping with various nonlinear structures: numerical evidences. *Nonlinear Dynamics*, 40:281–307, 2005.

[7] E. Gourdon and C.H. Lamarque. Nonlinear energy sink with uncertain parameters. *Journal of Computational and Nonlinear Dynamics*, 1:187–195, 2006.

[8] X. Jang, D.M. McFarland, L.A. Bergman, and A.F. Vakakis. Steady state passive nonlinear energy pumping in coupled oscillators: theoretical and experimental results. *Nonlinear Dynamics*, 33:87–102, 2003.

[9] J. N. Kapur and H. K. Kesavan. *Entropy optimization principles with applications*. Academic Press, San Diego, 1992.

[10] G. Kerschen, Y.S. Lee, A.F. Vakakis, D.M. McFarland, and L.A. Bergman. Irreversible passive energy transfer in coupled oscillators with essential nonlinearity. *Journal of Applied Mathematics*, 66:648–679, 2006.

[11] G. Kerschen, A.F. Vakakis, Y.S. Lee, D.M. McFarland, J.J. Kowtko, and L.A. Bergman. Energy transfers in a system of two coupled oscillators with essential nonlinearity: 1:1 resonance manifold and transient bridging orbits. *Nonlinear Dynamics*, 42:283–303, 2005.

[12] D.M. McFarland, L.A. Bergman, and A.F. Vakakis. Experimental study of non-linear energy pumping occurring at a single fast frequency. *International Journal of Non-Linear Mechanics*, 40:891–899, 2005.

[13] T.P. Sapsis, A.F. Vakakis, and L.A. Bergman. Effect of stochasticity on targeted energy transfer from a linear medium to a strongly nonlinear attachment. *Probabilistic Engineering Mechanics*, 2010.

[14] F. Schmidt and C.-H. Lamarque. Computation of the solutions of the fokker planck equation for one and two dof systems. *Communications in Nonlinear Science and Numerical Simulation*, 14:529, 2009.

[15] R. Serfling. *Approximation theorems of mathematical statistics*. Wiley, 1980.

[16] C. E. Shannon. A mathematical theory of communication. *Bell System Tech. J.*, 27:379–423,623–659, 1948.

[17] A.F. Vakakis and O.V. Gendelman. Energy pumping in nonlinear mechanical oscillators: Part II - Resonance capture. *Journal of Applied Mechanics*, 68:42–48, 2001.

[18] A.F. Vakakis, O.V. Gendelman, L.A. Bergman, D.M. McFarland, G. Kerschen, and Y.S. Lee. *Nonlinear targeted energy transfer in mechanical and structural systems*, volume 156 of *Solid mechanics and its applications*. Springer, 2008.

[19] A.F. Vakakis, L.I. Manevitch, O.V. Gendelman, and L.A. Bergman. Dynamics of linear discrete systems connected to local, essentially non-linear attachments. *Journal of Sound and Vibration*, 264:559–577, 2003.